HHS Public Access

Author manuscript

J Mol Neurosci. Author manuscript; available in PMC 2016 August 01.

Published in final edited form as:

J Mol Neurosci. 2015 August ; 56(4): 829–839. doi:10.1007/s12031-015-0518-5.

Role of astrocytes in leptin signaling

Yuping Wang[1], **Hung Hsuchou**[1], **Yi He**[1], **Abba J. Kastin**[1], and **Weihong Pan**[1,2,*]

[1]Blood-Brain Barrier Group, Pennington Biomedical Research Center, Baton Rouge, LA 70808

[2]Biopotentials Sleep Center, Baton Rouge, LA 70809

Abstract

To test the hypothesis that astrocytic leptin signaling induces an overall potentiation of the neuronal response to leptin, we generated a new line of astrocyte-specific leptin receptor knockout (ALKO-Δ1) mice in which no leptin receptor is expressed in astrocytes. Corresponding to cell-specific cre-recombinase expression in hypothalamic astrocytes but not neurons, this new strain of ALKO mice had attenuated pSTAT3 signaling in the arcuate nucleus of the hypothalamus 30 min after intracerebroventricular delivery of leptin. In response to high fat diet for two months, the ALKO mice showed a greater increase of percent fat and blood leptin concentration. This coincided with a mild reactive gliosis in the hypothalamus. Overall, the absence of leptin receptors in astrocytes attenuated hypothalamic pSTAT3 signaling, induced a mild reactive morphology, and promoted the development of diet-induced obesity. We conclude that leptin signaling in astrocytes is essential for the homeostasis of neuroendocrine regulation in obesity.

Keywords

leptin; astrocyte; STAT3; reactive astrogliosis; obesity

Introduction

Existing results suggest that leptin signaling in astrocytes can modulate the metabolic response to high-fat diet (HFD), but the detailed mechanisms involved are not yet clear. Leptin is a neuroendocrine polypeptide hormone produced by fat tissue and released into blood. After reaching the cerebral circulation, leptin crosses the blood-brain barrier (BBB) by a selective transport system (Banks et al., 1996). Within the central nervous system, leptin has multiple sites of action, including the hypothalamus, where its inhibitory effect on the development and maintenance of obesity is exerted. Hyperleptinemia and leptin resistance are common features in most forms of adult-onset obesity. Leptin resistance is thought to be caused by the saturation of BBB transport of leptin and desensitization of neuronal leptin signaling. It is only in the past few years that non-neuronal leptin signaling in the CNS and its regulatory changes in obesity have been addressed (Pan et al., 2008a; 2011a; 2012b).

*Corresponding author: Weihong Pan, MD, PhD, Biopotentials Sleep Center, 8032 Summa Ave, Ste A, Baton Rouge, LA 70809, Tel. 225-223-6899; sleep@biopotentials.org.

DISCLOSURE STATEMENT: All authors have nothing to declare.

In the hypothalamus, leptin receptors (LepR) are present in neurons, astrocytes, and cerebral endothelial cells, and they show developmental changes in subtype distribution and levels of expression (Pan et al., 2008b). The neuronal predominance of LepR in lean mice is shifted in full-blown adult-onset obesity, with a strong predilection for astrocytic expression. This is seen in agouti viable yellow (A^{vy}) mice that have sustained inactivation of melanocortin signaling (Pan et al., 2008a), in diet-induced obesity (DIO) after 6–8 weeks of feeding with HFD (Hsuchou et al., 2009), and in pan-LepR knockout mice (Hsuchou et al., 2013; Wang et al., 2013). In these models, there is an increase of reactive astrogliosis in the hypothalamus.

This leads to the question whether the concurrent increase of astrocytic LepR is a parallel phenomenon, or whether there is a causal relationship. If causal, it is still to be determined whether astrogliosis upregulates LepR, or vice versa where overexpression of LepR promotes astrogliosis. To further test these possibilities, we mapped and quantified the pattern of leptin-induced activation of phosphorylated Signal Transducer and Activator of Signaling (STAT)-3 in the arcuate nucleus of the hypothalamus (Arc). The mice in the model used differ from any previous knockout mice in that astrocytic LepR is fully removed rather than mutated. This allows us to differentiate the potential effect of “ligand passing” by a membrane-bound, though non-signaling receptor used in previous studies (Pan et al., 2011b).

Materials and Methods

Generation of Exon 1-flanked astrocytic leptin receptor knockout (ALKO-Δ1) mice

To generate ALKO mice, we used a cre recombinase transgenic mouse under the control of a mouse glial fibrillary acidic protein (GFAP) promoter. The GFAP-cre mice were B6.Cg-Tg(Gfap-cre)73.12Mvs/J (Stock number 012886, Jackson Laboratory, Bar Harbor, MN) that contain a mouse GFAP promoter sequence directing expression of Cre recombinase (Garcia et al., 2004). The LepR-floxed mice were B6.129P2-*Lepr*^{tm1Rck}/J (Stock number 008327, Jackson Laboratory), with *loxP* sites on either side of exon 1 (Cohen et al., 2001). $GFAP^{cre/+}$ hemizygous transgenic mice and $LepR^{loxP/loxP}$ homozygote mice were bred for two generations. The hemizygotes of the F1 generation were backcrossed with LepR-floxed mice, to select the F2 generation of ALKO-Δ1 mice that express both GFAP-cre and LepR-floxed alleles on tail genotyping. The agarose gel electrophoresis of PCR products and genotyping primers are shown in figure 1A and table 1.

Immunohistochemistry (IHC) to determine the regional difference and specificity of astrocytic LepR deletion

Two groups of mice were studied: ALKO and wildtype (WT) mice, both male and female, at age 4 months (m) (n = 3/group). The mice were anesthetized and perfused intracardially with phosphate buffered saline (PBS) followed by 4% paraformaldehyde (PFA). Brain was post-fixed in PFA overnight, cryoprotected in 15% and then 30% sucrose, and stored embedded in HistoPrep at −80 °C until cryosectioning. Coronal sections of 40 μm thickness were obtained by use of a Cryostat. Matching sections from the ALKO and WT mice were permeabilized with Triton X-100, blocked with normal donkey serum, and incubated with

Cre recombinase and S100 β primary antibodies overnight at 4 °C followed by fluorescent conjugated secondary antibodies for 2 h at 23 °C, with thorough washes in between, as described previously (Pan et al., 2008a; Hsuchou et al., 2009). The primary antibodies and secondary antibodies are listed in table 2. Negative controls for single staining used sections incubated with secondary antibody only. Dual labeling controls included sections stained with one primary antibody only. The sections were thoroughly washed in PBS and mounted by use of ProlongGold anti-fading mounting medium, coverslipped, and sealed. Confocal imaging was acquired using identical parameters and post-acquisition processing for matching sections between the two groups.

Intracerebroventricular delivery of leptin

Two groups of mice were studied: ALKO and WT mice at about 4 months old (n = 7/group). The mice were fasted overnight, anesthetized by intraperitoneal injection of urethane, and their body temperature maintained by use of a heating blanket. Stereotaxic injection of recombinant mouse leptin (R & D Systems, Minneapolis, MN) was performed at about 13:00 h, 6 h after onset of the light cycle. The coordinates for the right lateral ventricle were: 1 mm lateral, 0.2 mm posterior, and 2.5 mm below the skull surface. The dose of leptin was 2.5 μg in 1 μl of PBS, delivered by use of a syringe pump at an infusion rate of 0.5 μl/min. The needle was withdrawn slowly 1 min after cessation of the infusion. At 30 min after the initiation of leptin infusion, mice were either perfuse-fixed for IHC (n = 4/group) or decapitated to obtain brain regions for WB after blood collection for serum ELISA (n = 3/group). For IHC, the mouse was perfused intracardially with PBS and then 4 % PFA. Brain sections were processed as described above and IHC for pSTAT3 was performed, along with co-immunostaining of cell phenotype markers. Neurons were immunostained by a HuC/D antibody, whereas astrocytes were demarcated by a GFAP antibody. Detailed antibody information is shown in table 2.

Feeding experiments and metabolic analysis

ALKO and WT mice were started with a 45% HFD or isocaloric control diet (CD) with 10 % fat (cat#12451 and 12450H, respectively, Research Diets, New Brunswick, NJ) at age 6 weeks (n = 8–10 mice/group for a total of 4 groups). Besides basal body weight, percent fat was determined by nuclear magnetic resonance (NMR Minispec, Brucker) as described previously (Pan and Kastin, 2007). Percent fat and lean mass were monitored monthly during the course of diet manipulation. At the time of the terminal study (2 months after being on the diet), mice were anesthetized without fasting. Arterial blood was collected into a prechilled tube on ice by cutting of a carotid artery at zeitgeber time of 4–9 h (11am – 4 pm). Serum was used for measurement of glucose, leptin, and soluble LepR levels by ELISA as described previously (Jayaram et al., 2013), and brain tissue from half of the mice in each group was randomly collected for WB or qPCR analysis.

Western blotting (WB) analysis

Two classes of proteins were analyzed: signaling proteins downstream to leptin activation and structural proteins reflecting cell phenotype. Hypothalamic tissue was lysed in the presence of complete protease inhibitor cocktail containing phosphatase inhibitor (Pierce, Rockford, IL). Protein concentration was determined by use of the BCA assay. Forty μg of

protein/well was resolved in 10 % SDS-PAGE, transferred to nitrocellulose membrane, blocked with 4 % BSA, incubated with primary antibodies at 4 °C overnight, thoroughly washed, and incubated with HRP-conjugated secondary antibodies at 23 °C for 1 h. The membranes were then incubated with enhanced chemiluminescent reagents, and the signals were developed on X-ray film in the dark with a Kodak X-Omat device. The antibodies and loading controls are indicated in table 3.

Statistics

Means are presented with their standard errors. The effects of ALKO and leptin treatment on signaling activation and gene expression were analyzed by two-way analysis of variance. The interactions of the two factors were also determined. The effects of ALKO and diet were determined by repeated measures analysis of variance, followed by the Bonferroni post-hoc test of individual time points within the group.

Results

Specificity and sensitivity of ALKO mutation

The presence and relative levels of PCR products for cre recombinase, WT LepR, and floxed LepR alleles from tail DNA genotyping are shown in figure 1A. To determine the presence of cre recombinase in astrocytes, S100β was used as an astrocytic phenotype marker. The cell density of S100β (+) cells was similar in WT and ALKO mice. In the Arc of the WT mice, there was no Cre recombinase immunoreactivity. WT mice serve as an ideal negative control to confirm the specificity of the Cre antibody for IHC. In the ALKO mice, cre recombinase was expressed almost homogenously throughout the hypothalamus. Confocal images showed that the expression of Cre was highly associated with S100β, with a specificity of 95.60 ± 2.28 % in serial section analyses of 3 mice. The Arc had a high efficacy of Cre expression in astrocytes, as indicated by 72.22 ± 1.67 % of the S100β (+) cells that co-localized with Cre staining (Fig. 1B). Thus, the results indicate that essentially all Cre expression in this area resided in mature astrocytes, and more than two-thirds of the astrocytes had Cre incorporation driven by the GFAP promoter.

Effects of ALKO mutation and HFD to modulate leptin-induced pSTAT3 activation in the hypothalamus

To determine the differential effects of WT and ALKO mice on leptin-induced pSTAT3 activation, anesthetized mice received icv injection of either PBS vehicle control (1 μl) or leptin (2.5 μg/μl). IHC was performed 30 min later. The WT mice showed a minimal basal level of pSTAT3 expression that resided sporadically in neurons, shown by HuC/D double-labeling. Leptin icv induced a robust increase of pSTAT3. The cells were mainly neuronal, as pSTAT3 was present in the nuclei of neurons within the Arc. Tanycytes along the third ventricle also showed pSTAT3 immunoreactivity. By contrast, ALKO mice had no pSTAT3 signal after PBS icv, and they showed fewer cells and a lower density of pSTAT3 in the Arc after leptin icv. The pSTAT3 (+) cells were mainly in HuC/D (+) neurons, and the tanycytes were not activated (Fig. 2A).

Among the pSTAT3 (+) cells, there was heterogeneity of the levels of signal intensity. Although most of the cells appeared to be neuronal shown by confocal microscopic analysis after double-labeling with HuC/D (Fig. 2A–B), co-localization analysis of pSTAT3 with the astrocytic marker GFAP showed that some of the brighter pSTAT3 cells were associated with GFAP (+) processes in WT mice (Fig. 2C–D). In ALKO mice, astrocytic pSTAT3 was no longer seen, the pSTAT3 signal was less intense, and the GFAP (+) cells showed more engorged morphology suggesting mild reactive astrogliosis (Fig. 2D). The results were replicated four times.

In the hypothalamic homogenate (n = 3/group), leptin treatment but not the ALKO mutation had a significant effect on pSTAT3 expression ($p < 0.005$) by two-way analysis of variance. Post-hoc tests showed that the increase of pSTAT3 in WT mice receiving leptin was greater than in those receiving PBS ($p < 0.01$). ALKO mice receiving leptin icv showed a trend of increase from ALKO mice with PBS icv ($p = 0.056$), but there the increase was less than in the WT mice after leptin icv ($p < 0.05$) (Fig. 3A–B). The increase of pSTAT3 contrasts with a lack of change of total STAT3, neuronal marker NeuN, or astrocytic marker GFAP (Fig. 3C–E), despite a mild gliotic morphology in the ALKO mice. The results were duplicated.

Effects of ALKO mutation and HFD on body weight and adiposity

When fed with CD, ALKO and WT mice had similar weight and fat percent from birth till at least age 3 months. HFD resulted in weight gain in the WT mice, significant at weeks 7 and 8 in comparison with the CD group. The ALKO mice on HFD gained a significant amount of weight earlier, starting at week 4. By week 6, the ALKO mice on the HFD weighted more than the WT mice on HFD ($p < 0.05$; Fig. 4A). The increase of adiposity was apparent at 4 weeks in all 4 groups. The % fat was higher in the HFD groups than their respective CD controls of the same strain at weeks 6 and 8 (Fig. 4B). When expressed as percent fat gain in comparison with the “week 0” control (when mice were 6 weeks old), the ALKO mice had a greater increase of % fat both on CD and HFD (Fig. 4C).

Effect of ALKO and HFD on serum biomarkers

Serum leptin concentration was affected by both strain ($p < 0.05$) and diet ($p < 0.005$). The ALKO mice had higher concentrations of serum leptin than the WT mice while on the HFD ($p < 0.05$) (Fig. 5A). Serum sLepR level was only affected by diet ($p < 0.05$ for overall effect) but not by strain (Fig. 5B). By contrast, non-fasting blood glucose levels at 10 am showed a significant overall increase in the ALKO mice ($p < 0.05$). However, there was no main effect of diet or post-hoc difference (Fig. 5C).

Effect of ALKO and HFD on reactive astrogliosis

The ALKO mutation did not change overall GFAP expression by WB quantification while the mice were on the CD. This is similar to that seen in the leptin icv study shown above. However, ALKO mice on the HFD had a greater expression of GFAP than their WT counterpart ($p < 0.05$). This suggests an increase of reactive astrogliosis. However, the expression of cyclooxygenase (COX)-2 did not show major changes (Fig. 6). This suggests a lack of acute inflammatory changes in COX2 pathways.

Discussion

We have shown that obesity induces upregulation of astrocytic LepR, and that inhibition of astrocytic metabolic activity enhances neuronal leptin signaling in the A^{vy} mice with adult-onset obesity (Pan et al., 2008a). There are several possible mechanisms by which astrocytic LepR exerts its effects: (a) endocytose and process leptin; (b) transmit secondary signals to neurons; and (c) compete with neurons for the availability of leptin. Many of the questions can be addressed in experimental conditions in which astrocytes no longer express LepR. Here, we used astrocytic LepR knockout mice to identify potential mechanisms by which leptin signaling in astrocytes affects the cell-cell communication and the response of mice to DIO.

We first determined the specificity of LepR deletion in astrocytes by double labeling of cre recombinase with cell phenotype markers. Although GFAP-cre is the most reliable tool to drive cre recombinase expression in astrocytes, a small percent of neural progenitor cells also express GFAP at the embryonic stage (Casper et al., 2007). Thus, GFAP-cre mediated removal of the floxed gene would cause gene deletion in a few neurons in some CNS regions. Although the generation of inducible KO mice is a theoretical option, the technical feasibility of obtaining inducible ALKO in the 1:8 ratio is very low, particularly with the known information that there are additional challenges to produce inducible KO mice in astrocytes (Casper et al., 2007; Chow et al., 2008). Nonetheless, double-labeling IHC in the hypothalamus of the ALKO mice showed that cre recombinase was almost exclusively present in cells expressing S100β, another marker for astrocytes. The results indicate that the ALKO mice are suitable to study the effect of embryonic astrocytic LepR deletion on leptin-induced cell signaling in the hypothalamus.

In the Arc of the WT mice, pSTAT3 induction 30 min after leptin icv was mainly seen in cells expressing HuC/D, a marker of mature neurons, and in β1 tanycytes along the wall of the third ventricle. Like the WT mice receiving PBS icv, the ALKO mice receiving PBS did not have many pSTAT3 (+) cells. Leptin-induced pSTAT3 activation was seen in far fewer neurons and tanycytes in ALKO mice. Some of the cells with higher pSTAT3 intensity in WT mice receiving leptin were no longer seen in the ALKO mice. GFAP (+) astrocytes remained free of pSTAT3 activation. WB confirmed the overall reduction of pSTAT3 in response to leptin. Thus, a lack of astrocytic LepR attenuated the effect of leptin to induce cell signaling in both the number of neurons and also the intensity of activation. The effect was selective, rather than resulting from non-specific deletion of LepR from neurons. The results support a potentiating effect of astrocytic leptin signaling on the neuronal response to leptin. Since the GFAP (+) astrocytes appeared to be mildly gliotic with engorged cellular processes, a mechanism by which a lack of LepR results in astrocytic inflammation affecting neuronal pSTAT3 signaling might be involved, and an effect of ALKO on direct cell-cell communication between astrocytes and neurons is also possible.

GFAP is a protein expressed mainly by astrocytes. The GFAP promoter typically drives gene expression in astrocytes, though a small percent of neural progenitor cells also express GFAP at the embryonic stage (Casper et al., 2007; Garcia et al., 2004). To determine how astrocyte-specific leptin signaling modulates metabolic behavior, we initially generated a

strain of ALKO mice by cross-breeding the GFAP-cre recombinase transgenic mice with LepR-floxed mice (McMinn et al., 2004; Hsuchou et al., 2011). These ALKO-Δ17 mice, so called because the loxP sites flank exon 17 of LepR that encodes the membrane juxtapositional cytoplasmic domain (McMinn et al., 2004) have similar body weight and adiposity as their WT littermates fed with either CD or HFD (Jayaram et al., 2013). Nonetheless, ALKO-Δ17 mice have less leptin production, lower levels of circulating soluble LepR and triglyceride, reduced hypothalamic astrogliosis, and higher production of uncoupling protein UCP-1 in brown adipose tissue than their WT littermates under HFD. The better preserved biochemical profile in the ALKO-Δ17 mice suggests that astrocytic LepR signaling worsens obesity, a role counter to that of neuronal LepR (Jayaram et al., 2013). The results differ from the diabesity of neuronal LepR knockout mice (Kowalski et al., 2001; McMinn et al., 2005), but are more congruous with the endothelial LepR mutant mice that also produce a mutant, membrane-bound LepR in endothelia and show partial resistance to DIO (Pan et al., 2012a).

In previous studies with ALKO-Δ17 mice, a potential confounding factor prevented concluding a promoting role of astrocytic leptin signaling in the development of obesity. Present in the ALKO-Δ17 mice is a mutant membrane-bound LepR in astrocytes (Philo et al., 1994; Jayaram et al., 2013). It has been shown in cultured cells that a tail-less, membrane-bound LepR retains its capacity to endocytose leptin (Tu et al., 2010). Astrocytes in ALKO-Δ17 mice are predicted to internalize and possibly transcytose leptin, and perhaps generate secondary signaling to affect neuronal function.

Thus, we used an alternative approach to generate a new strain of ALKO mice that does not produce any LepR. This involved a different strain of LepR-floxed mice (Cohen et al., 2001) in which loxP sites flank exon 1 of LepR that encodes the N-terminus of the extracellular domain, instead of exon 17 that encodes the membrane juxtapositional cytoplasmic domain. When the LepR exon 1 floxed mice are back-crossed with cell specific cre-recombinase transgenic heterozygotes for two generations, about one-fourth of the F2 mice have neither soluble nor membrane-bound LepR in the targeted cells. With these newly generated ALKO-Δ1 mice used in the present report, we observed a different phenotype in response to HFD, suggesting that the membrane-bound, non-signaling mutant LepR in ALKO-Δ17 mice actually had an effect to modulate the fate of leptin in the brain.

The consequence of the ALKO-Δ1 mutation on the basal metabolic phenotype does not appear very large. This is consistent with a homeostatic regulatory role of astrocytes. Leptin does activate several other signaling pathways besides pSTAT3 downstream to the longest LepRb isoform, and there was some heterogeneity of receptor isoform composition and distribution in different regions of the hypothalamus and the entire brain. Alternative cellular signaling pathways might also show adaptive changes as a consequence of a lack of pSTAT3 signaling in response to leptin, though we did not detect changes of signals such as cyclin-dependent kinase-5 or its kinases that can be activated by leptin treatment (He et al., 2009). When fed with CD, ALKO mice had similar body weight, percent fat, fasting glucose, and blood leptin and sLepR levels as did the WT mice, at least up to 3 months of age. Upon HFD challenge (45% HFD in comparison with isocaloric controls), both ALKO and WT mice had an increase of adiposity after a month, and this progressed after 2 months.

By 8 weeks, however, the ALKO mice had a higher fat gain in comparison with the baseline. Blood leptin concentrations were higher, though sLepR was equally reduced in both strains. The protein expression of GFAP was increased in the hypothalamus. It appears that there was no major increase of inflammation (same level of COX-2) despite an increase of GFAP in ALKO mice on HFD. However, the mice showed less resilience to DIO than did ALKO-Δ17 in comparison with its FVB counterpart (Jayaram et al., 2013).

The difference between the ALKO-Δ1 mice in this study and the ALKO-Δ17 mice in our previous report (Jayaram et al., 2013) might be largely explained by sLepR that serves as a leptin antagonist (Yang et al., 2004; Tu et al., 2008). In addition, astrocytes from the ALKO-Δ17 mice continue to endocytose leptin, and may serve either as a reservoir or a competing compartment of leptin reaching the adjacent neurons. It is clear that astrocytic leptin signaling directly affects neuronal pSTAT3 activation and the response of mice to DIO.

In summary, we present for the first time a new strain of ALKO mice devoid of LepR in their astrocytes. The specificity of ALKO was verified by cre recombinase IHC, and the reduction of leptin-induced pSTAT3 activation was shown by IHC and WB. In response to 45% HFD, the ALKO mice had greater fat gain and hyperleptinemia and increased GFAP expression. Overall, part of the effect of leptin on neuroendocrine regulation is mediated by astrocytes.

Acknowledgments

Grant support was provided by NIH (DK54880, DK92245, NS62291). Cryosectioning was performed in the Cell Biology and Cell Imaging Core Facility with service charge.

References

Banks WA, Kastin AJ, Huang W, Jaspan JB, Maness LM. Leptin enters the brain by a saturable system independent of insulin. Peptides. 1996; 17:305–311. [PubMed: 8801538]

Casper KB, Jones K, McCarthy KD. Characterization of astrocyte-specific conditional knockouts. Genesis. 2007; 45:292–299. [PubMed: 17457931]

Chow LM, Zhang J, Baker SJ. Inducible Cre recombinase activity in mouse mature astrocytes and adult neural precursor cells. Transgenic Res. 2008; 17:919–928. [PubMed: 18483774]

Cohen P, Zhao C, Cai X, Montez JM, Rohani SC, Feinstein P, Mombaerts P, Friedman JM. Selective deletion of leptin receptor in neurons leads to obesity. J Clin Invest. 2001; 108:1113–1121. [PubMed: 11602618]

Garcia AD, Doan NB, Imura T, Bush TG, Sofroniew MV. GFAP-expressing progenitors are the principal source of constitutive neurogenesis in adult mouse forebrain. Nat Neurosci. 2004; 7:1233–1241. [PubMed: 15494728]

He Y, Kastin AJ, Hsuchou H, Pan W. The Cdk5/p35 kinases modulate leptin-induced STAT3 signaling. J Mol Neurosci. 2009; 39:49–58. [PubMed: 19156541]

Hsuchou H, He Y, Kastin AJ, Tu H, Markadakis EN, Rogers RC, Fossier PB, Pan W. Obesity induces functional astrocytic leptin receptors in hypothalamus. Brain. 2009; 132:889–902. [PubMed: 19293246]

Hsuchou H, Kastin AJ, Tu H, Markadakis EN, Stone KP, Wang Y, Heymsfield SB, Chua SC Jr, Obici S, Magrisso IJ, Pan W. Effects of cell type-specific leptin receptor mutation on leptin transport across the BBB. Peptides. 2011; 32:1392–1399. [PubMed: 21616110]

Hsuchou H, Wang Y, Cornelissen-Guillaume GG, Kastin AJ, Jang E, Halberg F, Pan W. Diminished leptin signaling can alter circadian rhythm of metabolic activity and feeding. J Appl Physiol. 2013; 115:995–1003. [PubMed: 23869060]

Jayaram B, Pan W, Wang Y, Hsuchou H, Mace A, Cornélissen GG, Mishra PK, Koza RA, Kastin AJ. Astrocytic leptin receptor knockout mice show partial rescue of leptin resistance in diet-induced obesity. J Appl Physiol. 2013; 114:734–741. [PubMed: 23329815]

Kowalski TJ, Liu SM, Leibel RL, Chua SC Jr. Transgenic complementation of leptin-receptor deficiency. I. Rescue of the obesity/diabetes phenotype of LEPR-null mice expressing a LEPR-B transgene. Diabetes. 2001; 50:425–435. [PubMed: 11272157]

McMinn JE, Liu SM, Dragatsis I, Dietrich P, Ludwig T, Eiden S, Chua SC Jr. An allelic series for the leptin receptor gene generated by CRE and FLP recombinase. Mamm Genome. 2004; 15:677–685. [PubMed: 15389315]

McMinn JE, Liu SM, Liu H, Dragatsis I, Dietrich P, Ludwig T, Boozer CN, Chua SC Jr. Neuronal deletion of Lepr elicits diabesity in mice without affecting cold tolerance or fertility. Am J Physiol Endocrinol Metab. 2005; 289:E403–E411. [PubMed: 15870101]

Pan W, Hsuchou H, Cornelissen-Guillaume GG, Jayaram B, Wang Y, Tu H, Halberg F, Wu X, Chua SC Jr, Kastin AJ. Endothelial leptin receptor mutation provides partial resistance to diet-induced obesity. J Appl Physiol. 2012a; 112:1410–1418. [PubMed: 22323652]

Pan, W.; Hsuchou, H.; He, Y.; Kastin, AJ. The astroglial leptin receptors and obesity. In: Preedy, VR., editor. Modern Insights into Disease - from Molecules to Man: Adipokines. Enfield, NH, USA: Science Publishers; 2011a. p. 185-196.

Pan W, Hsuchou H, He Y, Sakharkar A, Cain C, Yu C, Kastin AJ. Astrocyte Leptin Receptor (ObR) and Leptin Transport in Adult-Onset Obese Mice. Endocrinology. 2008a; 149:2798–2806. [PubMed: 18292187]

Pan W, Hsuchou H, Jayaram B, Khan RS, Huang EYK, Wu X, Chen C, Kastin AJ. Leptin action on non-neuronal cells in the CNS: potential clinical implications. Ann N Y Acad Sci. 2012b; 1264:64–71. [PubMed: 22530983]

Pan W, Hsuchou H, Tu H, Kastin AJ. Developmental changes of leptin receptors in cerebral microvessels: unexpected relation to leptin transport. Endocrinology. 2008b; 149:877–885. [PubMed: 18039787]

Pan W, Hsuchou H, Xu CL, Wu X, Bouret SG, Kastin AJ. Astrocytes modulate distribution and neuronal signaling of leptin in the hypothalamus of obese A^{vy} mice. J Mol Neurosci. 2011b; 43:478–484. [PubMed: 21086065]

Pan W, Kastin AJ. Mahogany, blood-brain barrier, and fat mass surge in A^{vy} mice. International Journal of Obesity. 2007; 31:1030–1032. [PubMed: 17224930]

Philo J, Talvenheimo J, Wen J, Rosenfeld R, Welcher A, Arakawa T. Interactions of neurotrophin-3 (NT-3), brain-derived neurotrophic factor (BDNF), and the NT-3·BDNF heterodimer with the extracellular domains of the TrkB and TrkC receptors. J Biol Chem. 1994; 269:27840–27846. [PubMed: 7961713]

Tu H, Hsuchou H, Kastin AJ, Wu X, Pan W. Unique leptin trafficking by a tailless receptor. FASEB J. 2010; 24:2281–2291. [PubMed: 20223942]

Tu H, Kastin AJ, Hsuchou H, Pan W. Soluble receptor inhibits leptin transport. J Cell Physiol. 2008; 214:301–305. [PubMed: 17620316]

Wang Y, He J, Kastin AJ, Hsuchou H, Pan W. Hypersomnolence and reduced activity in pan-leptin receptor knockout mice. J Mol Neurosci. 2013; 51:1038–1045. [PubMed: 23955775]

Yang G, Ge H, Boucher A, Yu X, Li C. Modulation of direct leptin signalling by soluble leptin receptor. Mol Endocrinol. 2004; 18:1354–1362. [PubMed: 15016839]

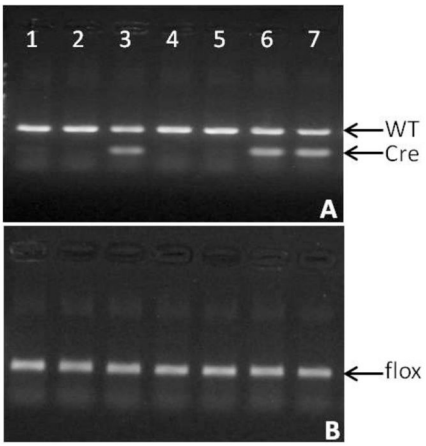

Fig. 1A

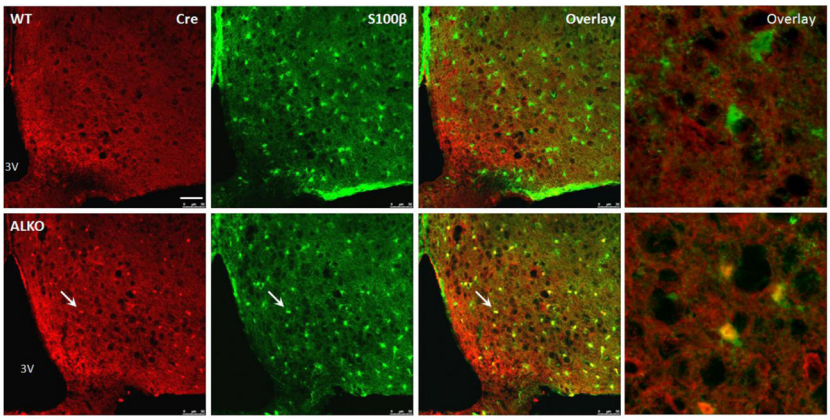

Fig.1B

Fig. 1.

Specificity of ALKO-Δ1 mutation. (A) Tail DNA genotyping showed that the ALKO mice (lanes 3, 6, and 7) had a WT GFAP PCR product of 324 bp, a cre recombinase transgene amplicon of 100 bp, and floxed LepR amplicon of 227 bp. (B) Confocal microscopic images of sections of the arcuate nucleus of the hypothalamus (Arc). The WT mouse (top row) did not show cre recombinase immunoreactivity. The ALKO mouse (bottom row) showed overlap of cre recombinase immunoreactivity (red) and an astrocytic marker S100β (green) in the same cells. Scale bar of first 3 columns: 50 μm. Scale bar of the last column: 5 μm.

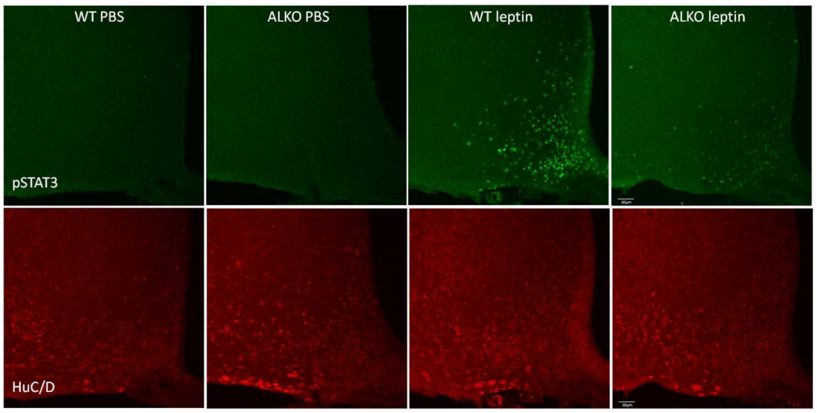

Fig. 2A

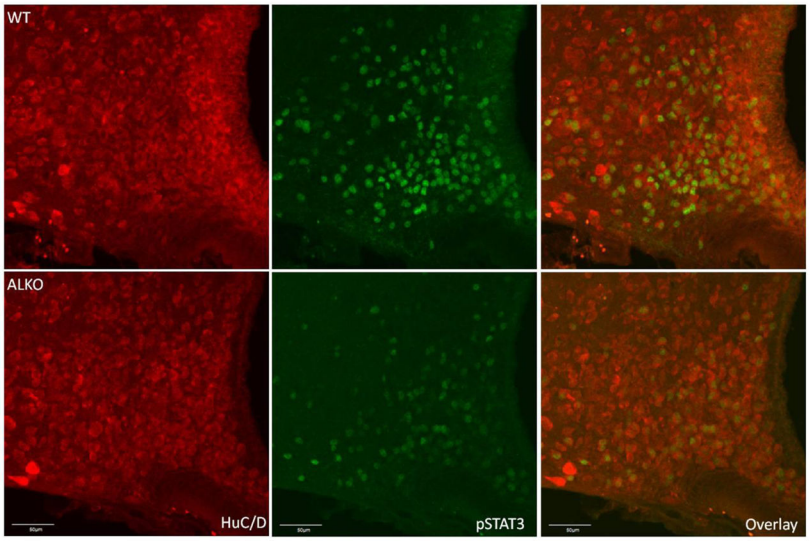

Fig. 2B

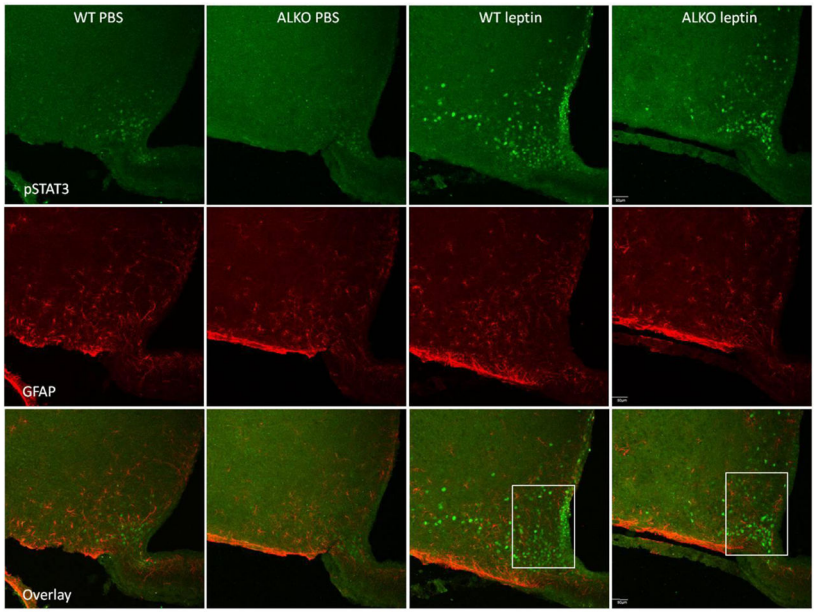

Fig.2C

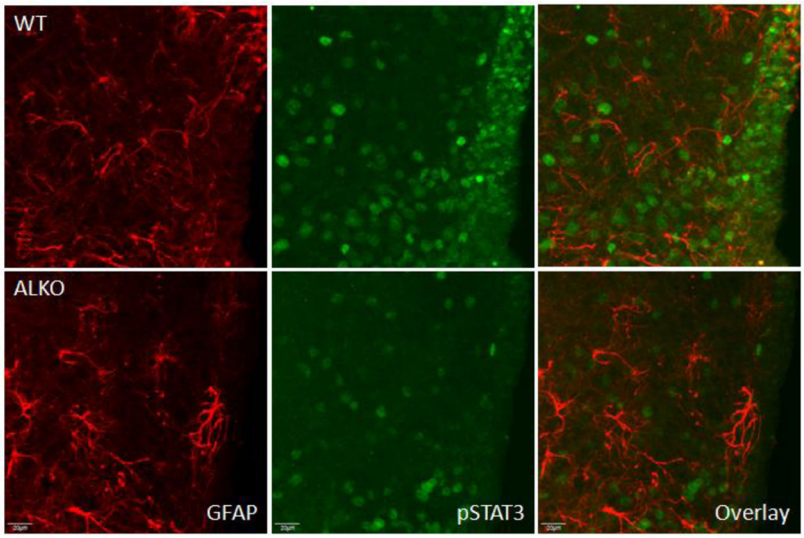

Fig.2D

Fig. 2.

Effect of ALKO on cell-type specific pSTAT3 activation in Arc region 30 min after leptin icv. (A) While the basal level of pSTAT3 immunoreactivity was minimal in both WT and ALKO mice after PBS icv, WT responded to leptin with robust pSTAT3 activation in cells that also expressed the neuronal marker HuC/D. ALKO mice did not have the same level of pSTAT3 activation. (B) Higher magnification images showing co-localization of pSTAT3 and HuC/D by confocal microscopy. Scale bar: 50 μm. (C) In slightly more rostral sections, pSTAT3 activation is seen in ArC neurons and tanycytes along the third ventricle of the WT mice after leptin icv, with minimal overlap with GFAP immunoreactivity. This was

attenuated in a matching section from an ALKO mouse, where the number of pSTAT3 (+) neurons was decreased and that of tanycytes was diminished. (D) Higher magnification images show that pSTAT3 immunoreactivity had heterogeneous intensity in a WT mouse that did not overlap with GFAP. The pSTAT3 signal was reduced and more homogeneous with low intensity in the ALKO mice. The GFAP staining depicts an increase of engorgement of astrocytes, suggesting mild reactivity. Scale bar: 20 μm.

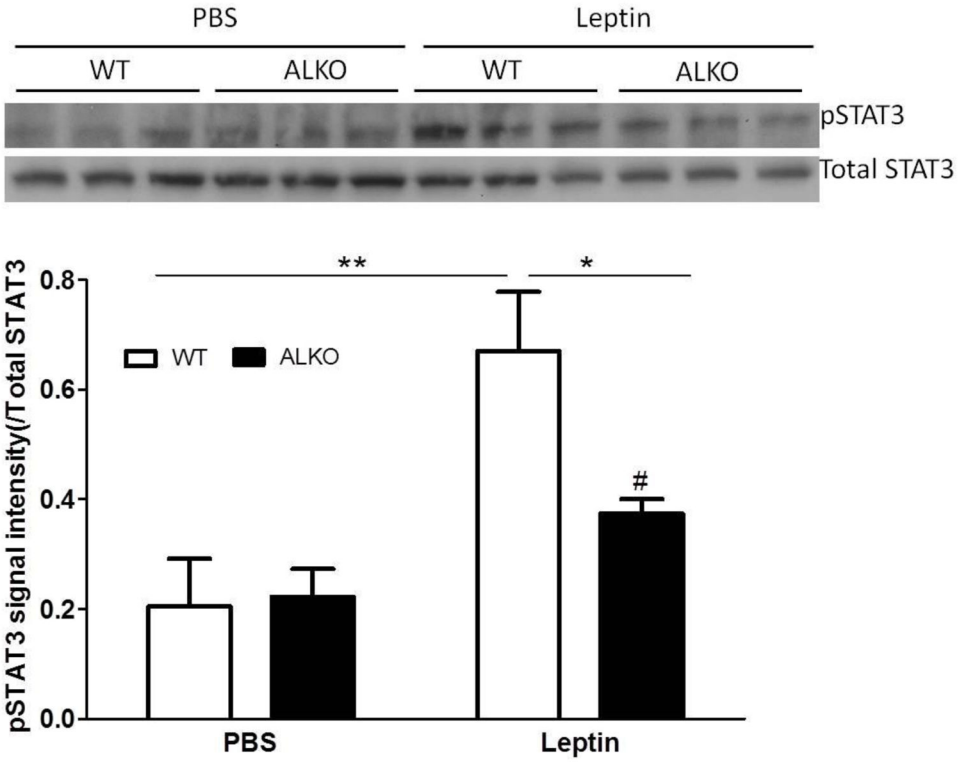

Fig.3A and Fig.3B

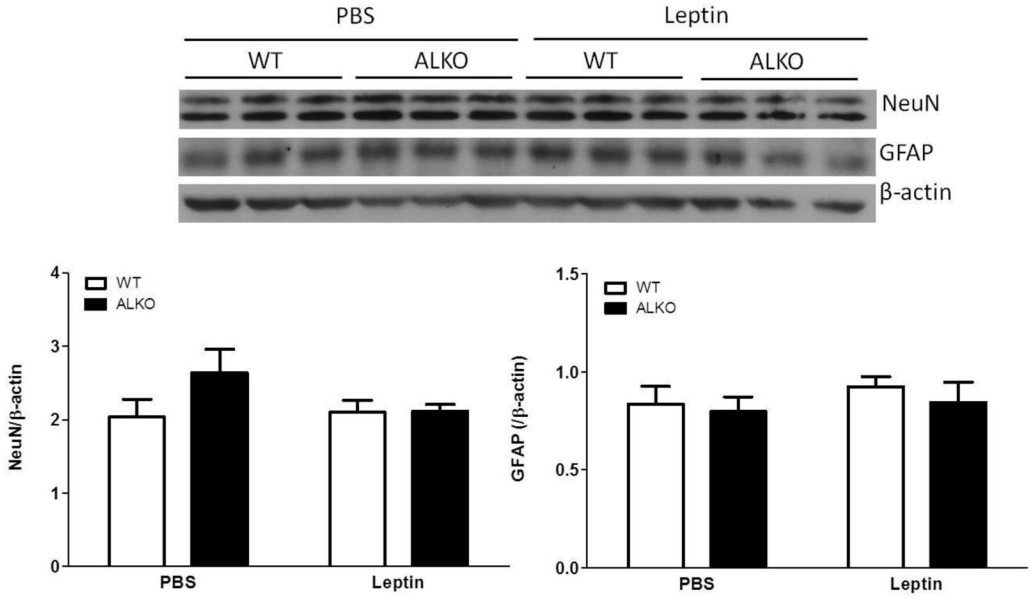

Fig.3C , 3D , 3E

Fig. 3.

Effects of ALKO and leptin icv on hypothalamic pSTAT3 signaling. (A) In WT mice, leptin icv induced an increase of pSTAT3 signal intensity at 30 min. In ALKO mice, the basal low level of pSTAT3 was similar to that of WT mice, and the leptin-induced increase was less pronounced than that of WT. (B) Densitometric analysis showed that pSTAT3 was increased significantly in the WT but not ALKO mice (n = 3/group). *: $p < 0.05$; **: $p < 0.01$; #: $p = 0.07$. (C) The expression of neuronal marker NeuN and astrocytic marker GFAP did not change as a result of ALKO or leptin icv. (D) Densitometric analysis of NeuN expression showing a lack of significant change. (E) Densitometric analysis of GFAP expression showing a lack of significant change by ALKO or leptin icv.

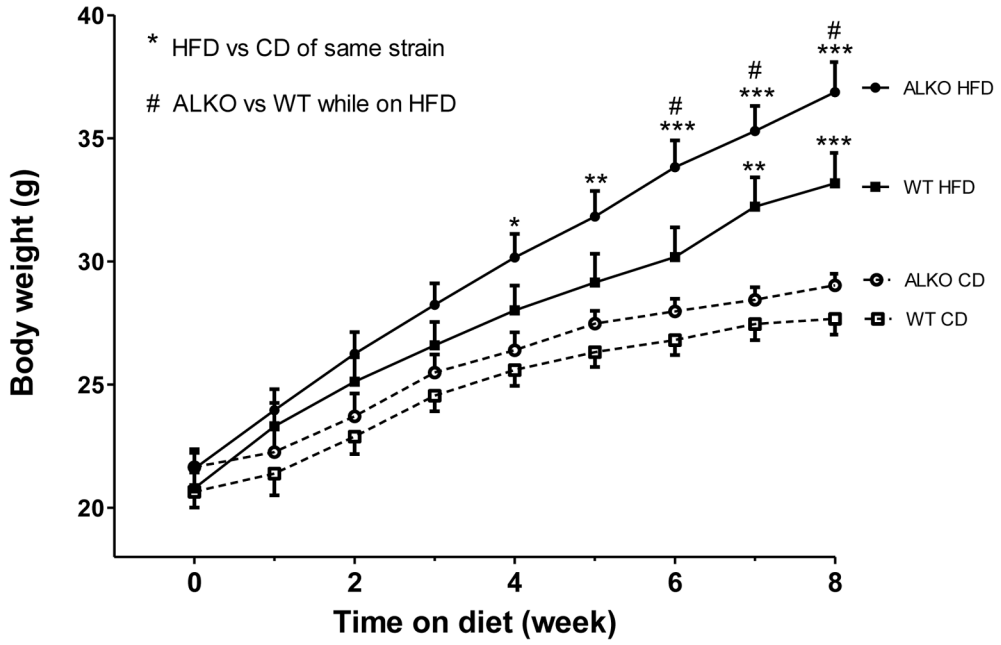

Fig.4A

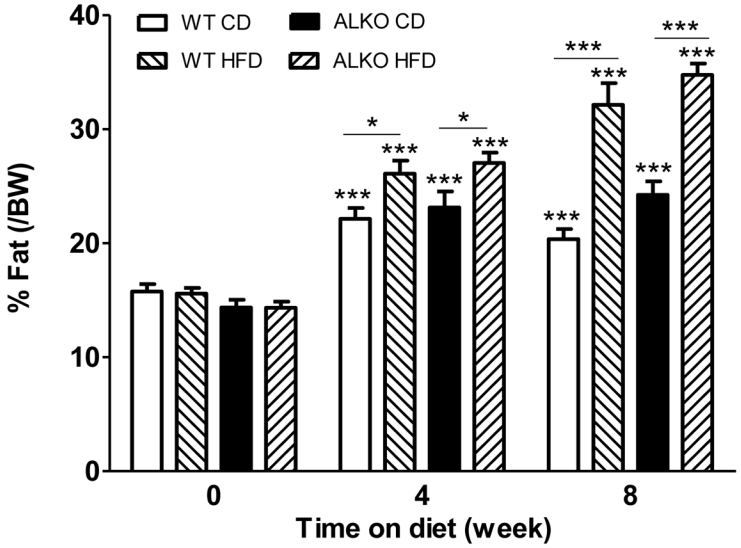

Fig.4B

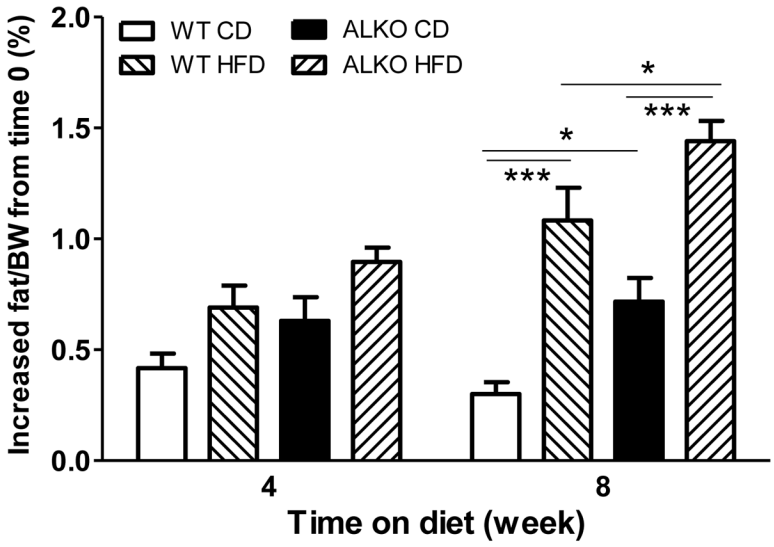

Fig.4C

Fig. 4.

Response of ALKO-Δ1 mice to 45% HFD. (A) Since starting the experimental diet at the age of 4 weeks, ALKO and WT littermates had similar weight gain on control diet (CD). Both strains gained more weight on HFD in comparison with their respective CD groups. ALKO HFD gained more weight than the WT HFD group at 6 – 8 weeks of HFD feeding. (B) %fat was increased after 4 weeks of HFD in both ALKO and WT mice, and this persisted at 8 weeks. (C) The increase of %fat, in comparison with time 0 (4 week old), was significantly higher in the ALKO mice at 8 weeks of diet, including both CD and HFD groups (n = 8–10 mice/group). *: $p < 0.05$; **: $p < 0.01$; ***: $p < 0.005$.

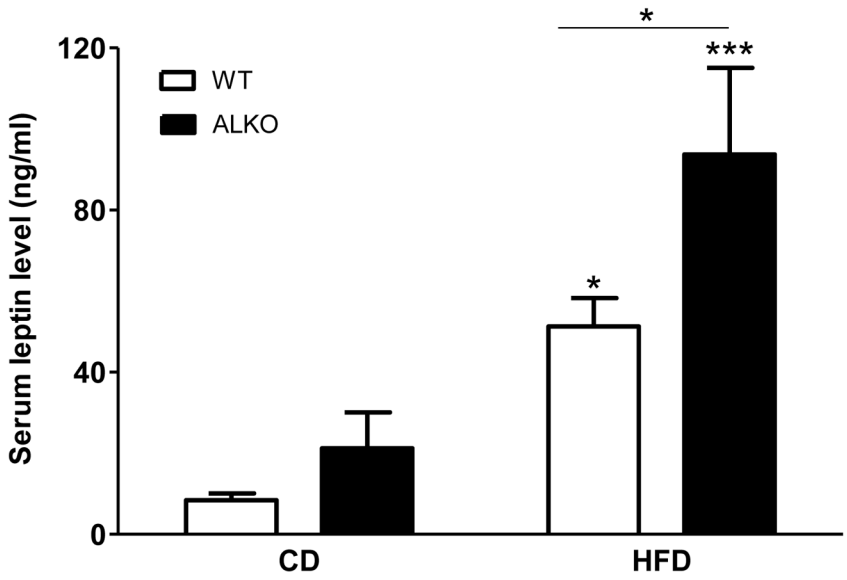

Fig.5A

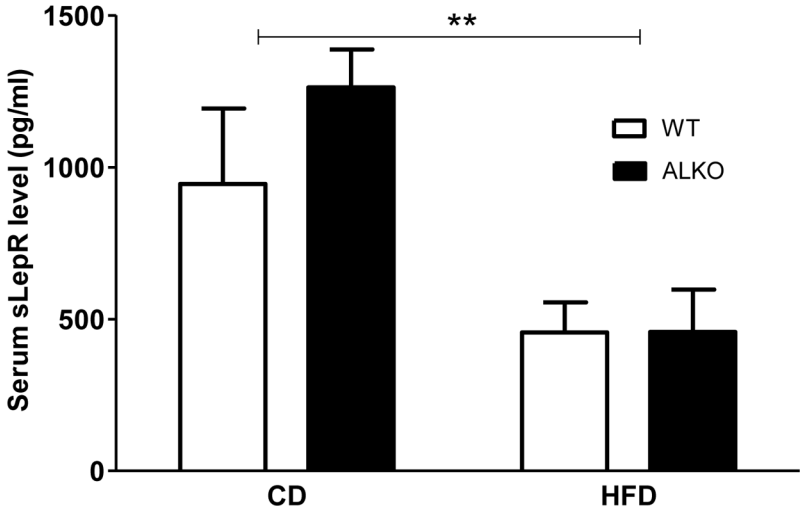

Fig.5B

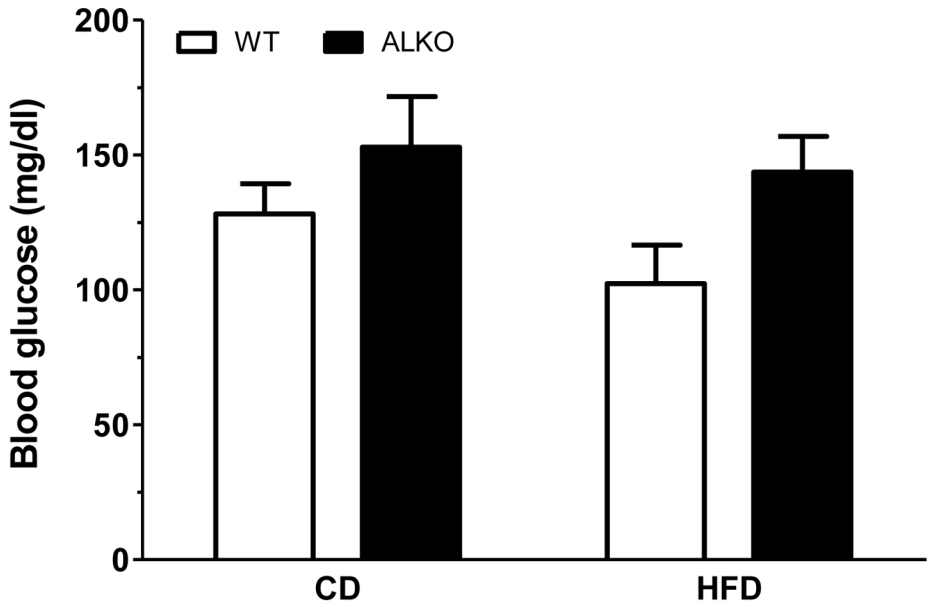

Fig.5C

Fig. 5.

Effect of ALKO and HFD on serum biomarkers of obesity. (A) Leptin concentrations were increased after 8 weeks of HFD. The increase was greater in ALKO mice than WT mice. (B) sLepR level was similar in the WT and ALKO mice. There was a significant decrease by HFD in both strains. (C) Fasting blood glucose concentrations did not show significant change by strain or diet at this time (n = 6/group). *: $p < 0.05$; **: $p < 0.01$; ***: $p < 0.005$.

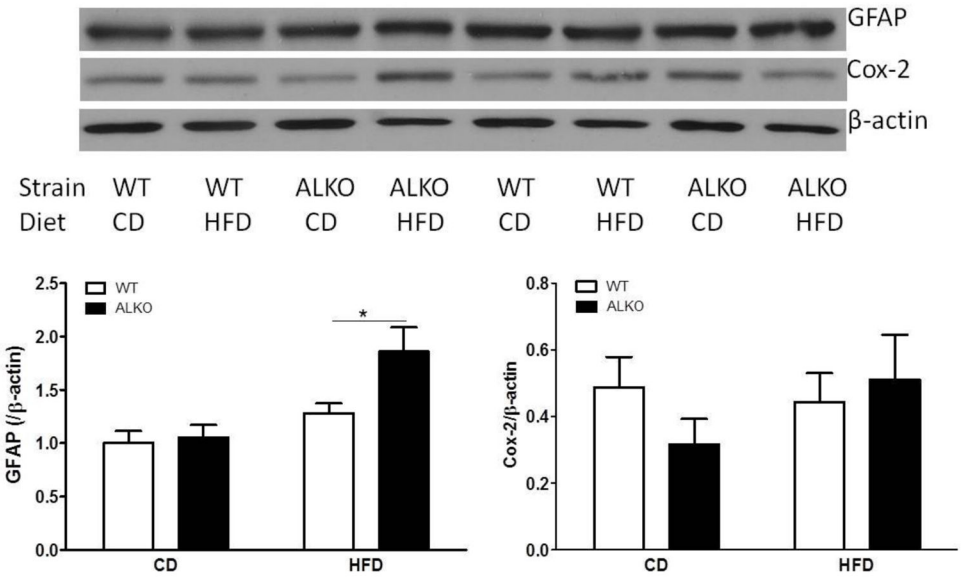

Fig. 6.

Potential effects of ALKO and HFD on reactive astrogliosis. (A) WB of 4 groups of hypothalamic samples (n = 2/group) showed that GFAP expression was mainly increased by HFD in the ALKO mice, though (B) there were both strain and diet effects by two-way ANOVA. (C) COX-2 protein expression did not change by diet or ALKO mutation. *: $p < 0.05$.

Table 1

Genotyping primers

Gene	Forward primer	Reverse primer	Amplicon size
GFAP-cre WT	5′-CTAGGCCACAGAATTGAAAGATCT	5′-GTAGGTGGAAATTCTAGCATCATCC	324 bp
GFAP-cre transgene	5′-GCGGTCTGGCAGTAAAAACTATC	5′-GTGAAACAGCATTGCTGTCACTT	100 bp
LepR-floxed	5′-GTCACCTAGGTTAATGTATTC	5′-TCTAGCCCTCCAGCACTGGAC	227 bp

Table 2

Antibodies used for IHC

Antibody	Host species	Dilution	Company
pSTAT3 (Tyr^{705})	Rabbit	1:100	Cell Signaling Technology
HuC/D	Mouse	1:100	Life Technology
GFAP	Mouse	1:500	Sigma
Cre recombinase	Mouse	1:100	Abcam
S100β	Rabbit	1:100	Abcam
Alexa488 donkey anti-rabbit 2° Ab	Donkey	1:500	Life Technology
Alexa 594 donkey anti-mouse 2° Ab	Donkey	1:500	Life Technology

Table 3

Antibodies used for western blotting

Antibodies	Host species	Dilution	Company
pSTAT3 (Tyr^{705})	Rabbit	1:1000	Cell Signaling Technology
Total STAT3	Rabbit	1:2000	Cell Signaling Technology
NeuN	Mouse	1:500	Millipore
GFAP	Rabbit	1:2000	Sigma
COX-2	Mouse	1:300	Santa Cruz Biotechnology
β-actin	Mouse	1:5000	Sigma
HRP-conjugated anti-mouse 2° Ab	Goat	1:5000	Thermo Scientific
HRP-conjugated anti-rabbit 2° Ab	Goat	1:5000	Thermo Scientific